Atypical fracture with long-term bisphosphonate therapy is associated with altered cortical composition and reduced fracture resistance

Ashley A. Lloyd[a], Bernd Gludovatz[b], Christoph Riedel[c], Emma A. Luengo[a], Rehan Saiyed[d], Eric Marty[d], Dean G. Lorich[d,e,f], Joseph M. Lane[d,e,f], Robert O. Ritchie[g,h], Björn Busse[c], and Eve Donnelly[a,i,1]

[a]Department of Materials Science and Engineering, Cornell University, Ithaca, NY 14850; [b]School of Mechanical and Manufacturing Engineering, UNSW Sydney, NSW 2052, Australia; [c]Department of Osteology and Biomechanics, University Medical Center Hamburg, D-22529 Hamburg, Germany; [d]Department of Orthopedic Surgery, Hospital for Special Surgery, New York, NY 10021; [e]Orthopedic Surgery, Weill Medical College, Cornell University, New York, NY 10065; [f]Medical Orthopedic Trauma Service, NewYork–Presbyterian Hospital/Weill Cornell Medical Center, New York, NY 10065; [g]Materials Sciences Division, Lawrence Berkeley National Laboratory, Berkeley, CA 94720; [h]Department of Materials Science and Engineering, University of California, Berkeley, CA 94720; and [i]Research Division, Hospital for Special Surgery, New York, NY 10021

Edited by John T. Potts, Massachusetts General Hospital, Charlestown, MA, and approved June 29, 2017 (received for review March 18, 2017)

Bisphosphonates are the most widely prescribed pharmacologic treatment for osteoporosis and reduce fracture risk in postmenopausal women by up to 50%. However, in the past decade these drugs have been associated with atypical femoral fractures (AFFs), rare fractures with a transverse, brittle morphology. The unusual fracture morphology suggests that bisphosphonate treatment may impair toughening mechanisms in cortical bone. The objective of this study was to compare the compositional and mechanical properties of bone biopsies from bisphosphonate-treated patients with AFFs to those from patients with typical osteoporotic fractures with and without bisphosphonate treatment. Biopsies of proximal femoral cortical bone adjacent to the fracture site were obtained from postmenopausal women during fracture repair surgery (fracture groups, $n = 33$) or total hip arthroplasty (nonfracture groups, $n = 17$). Patients were allocated to five groups based on fracture morphology and history of bisphosphonate treatment [+BIS Atypical: $n = 12$, BIS duration: 8.2 (3.0) y; +BIS Typical: $n = 10$, 7.7 (5.0) y; +BIS Nonfx: $n = 5$, 6.4 (3.5) y; −BIS Typical: $n = 11$; −BIS Nonfx: $n = 12$]. Vibrational spectroscopy and nanoindentation showed that tissue from bisphosphonate-treated women with atypical fractures was harder and more mineralized than that from bisphosphonate-treated women with typical osteoporotic fractures. In addition, fracture mechanics measurements showed that tissue from patients treated with bisphosphonates had deficits in fracture toughness, with lower crack-initiation toughness and less crack deflection at osteonal boundaries than that of bisphosphonate-naïve patients. Together, these results suggest a deficit in intrinsic and extrinsic toughening mechanisms, which contribute to AFFs in patients treated with long-term bisphosphonates.

atypical fracture | bisphosphonates | subtrochanteric fracture | fracture toughness | FTIR imaging

Bisphosphonates, a widely prescribed class of antiresorptive drug that inhibits osteoclast-mediated bone resorption, play a key role in management of bone diseases including postmenopausal osteoporosis and skeletal metastases (1–3). Bisphosphonates minimize bone loss and reduce the risk of fracture in patients with postmenopausal osteoporosis (4, 5). However, in the last decade, long-term bisphosphonate treatment has been associated with side effects that include atypical femoral fractures (AFFs), rare, transverse fractures of the femoral shaft. The subtrochanteric cortical site and transverse morphology characteristic of a brittle fracture contrast with the cancellous site and intertrochanteric or femoral neck morphologies observed in typical fragility fractures at the hip (6, 7) (Fig. 1). Patient anxieties about side effects have contributed to a crisis in osteoporosis treatment arising from a 50% decrease in use of oral bisphosphonates between 2008 and 2012, raising the specter of a return to high rates of hip fracture previously thought to have been reduced following the widespread prescription of bisphosphonates for postmenopausal osteoporosis (8–10).

Thus, AFFs represent an apparent paradox in the treatment of osteoporosis. These catastrophic fractures are a rare side effect of a class of pharmacologic agents that, for the vast majority of patients, substantially reduces fracture risk. This complexity of treatment responses highlights a need for further understanding of how antiresorptive treatments modulate the properties of bone.

Prior studies examining the mechanical properties of bisphosphonate-treated bone have focused primarily on the role of turnover suppression in preventing bone loss at cancellous sites of typical osteoporotic fractures (4, 11, 12). In contrast, AFFs occur in cortical bone and seem to propagate through a stress fracture-like mechanism, suggesting that by reducing turnover bisphosphonates may impair toughening mechanisms in cortical bone, which act as important barriers to clinical fracture in healthy bone (7, 13). At the micro scale, bisphosphonate treatment can potentially impair toughening through several mechanisms: by decreasing osteonal density, which could alter extrinsic toughening by reducing crack deflection at osteonal interfaces (14–16); by reducing compositional heterogeneity, which potentially reduces

Significance

Since the first reports of atypical femoral fractures (AFFs), a clinical phenomenon in which patients experience catastrophic brittle fractures of the femoral shaft with minimal trauma, the risk associated with bisphosphonates, the most widely prescribed pharmaceuticals for osteoporosis, has become increasingly well-established. However, the underlying cause of AFFs and their causal relationship to bisphosphonates is unknown. Here we examine bone tissue from women with AFFs and show that long-term bisphosphonate treatment degrades the fracture-resistance toughening mechanisms that are inherent to healthy bone. Our work resolves the apparent paradox of AFFs as a side effect of the most common osteoporosis treatment by clarifying the differing effects of bisphosphonates on bone tissue structure and mechanical properties across multiple length scales.

Author contributions: A.A.L., J.M.L., R.O.R., B.B., and E.D. designed research; A.A.L., B.G., C.R., E.A.L., R.S., E.M., D.G.L., J.M.L., and E.D. performed research; A.A.L., B.G., C.R., E.A.L., R.S., E.M., and B.B. analyzed data; and A.A.L., R.O.R., and E.D. wrote the paper.

Conflict of interest statement: J.M.L. consults for Bone Therapeutics, SA, CollPlant, Ltd., Grafty's, Inc., Kuros Biosurgery AG, RadiusHealth, Inc., Terumo BCT, Inc., and Wright Medical Technology. All other authors declare no conflict of interest.

This article is a PNAS Direct Submission.

Freely available online through the PNAS open access option.

[1]To whom correspondence should be addressed. Email: eve.donnelly@cornell.edu.

This article contains supporting information online at www.pnas.org/lookup/suppl/doi:10.1073/pnas.1704460114/-/DCSupplemental.

www.pnas.org/cgi/doi/10.1073/pnas.1704460114

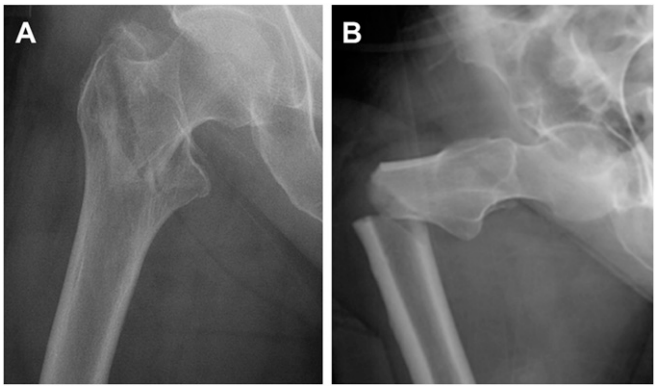

Fig. 1. Radiographs showing morphology of a typical intertrochanteric fragility fracture (*A*), compared with an AFF (*B*). Whereas the typical fracture has a tortuous crack path indicative of interaction with microstructural features that act as toughening mechanisms, the atypical fracture has a transverse morphology indicative of a brittle fracture process.

the intrinsic plasticity that nanoscale heterogeneity provides (17, 18); and by increasing nonenzymatic collagen cross-linking, which may lead to loss of postyield (intrinsic) toughness through reduced collagen fibrillar sliding (14, 19). Although each of these putative effects of bisphosphonate treatment has been observed separately, there has been no definitive demonstration that the combination of these degradation mechanisms on the fracture behavior of cortical bone can be directly linked to the origin of AFFs.

Since the first case reports of atypical fractures (20) many studies have addressed the epidemiology (21, 22), radiographic morphology (23, 24), and clinical management of atypical fractures (summarized in refs. 6 and 7). Compositional studies of bone from patients with AFFs showed that the femoral cortices had elevated mineralization relative to those with typical osteoporotic fractures (17). However, there has so far been no direct assessment of fracture properties of bone tissue in patients with AFFs, and few studies have differentiated altered tissue composition and mechanical properties arising from two key interrelated variables: bisphosphonate treatment and atypical fracture morphology.

Thus, the objectives of this study were (*i*) to assess the compositional and mechanical properties of biopsies from long-term bisphosphonate-treated patients with AFFs across several length scales and (*ii*) to compare these properties to those from patients with differing fracture morphologies and bisphosphonate treatment histories to discern the differential contributions of these variables to the measured bone tissue properties.

Results

Patient Characteristics. In the bisphosphonate-treated (+BIS) groups, duration of bisphosphonate treatment did not differ across groups (+BIS Atypical 8.3 ± 3.3 y; +BIS Typical 7.7 ± 5.0 y; +BIS Nonfx 6.4 ± 3.5 y; Table 1). The ages of the +BIS Atypical fracture patients were similar to those in the other groups ($P > 0.05$ +BIS Atypical vs. all other groups; Table 1). The −BIS Nonfx patients were younger than patients in both typical groups (−BIS Nonfx 71 ± 5.8 y vs. −BIS Typical 83 ± 4.9 y, $P = 0.013$; vs. +BIS Typical 81 ± 12 y, $P = 0.032$). Patient ages were similar across all other groups. A linear fixed effects model was used to isolate the effects of patient variables (fracture morphology and bisphosphonate treatment history) while adjusting for the effects of patient age on the measured geometric, microstructural, and mechanical properties (*Materials and Methods*).

Cortical Biopsies from Atypical Fracture Patients Show Increased Cortical Thickness and Reduced Intracortical Bone Volume Fraction Compared with Those from Typical Fracture Patients. Radiographs were used to assess cortical thickness and cortical ratio (ratio of cortical thickness to femoral diameter) at 30 mm and 100 mm distal to the lesser trochanter. At 30 mm distal to the lesser trochanter, femora from patients with atypical fractures had greater cortical thickness and cortical ratio compared with those from patients with typical fractures (Atypical medial thickness at 30 mm +18% vs. Typical, $P = 0.03$; lateral thickness at 30 mm +19% vs. Typical, $P = 0.05$; cortical ratio at 30 mm +19% vs. Typical, $P < 0.01$).

Femora from patients without fractures were also more robust overall than those from patients with typical or atypical fractures. Femora from nonfracture patients had greater cortical thickness and cortical ratio at both 30 mm and 100 mm distal to the lesser trochanter compared with femora from patients with typical fractures and greater cortical thickness and cortical ratio at 100 mm distal to the lesser trochanter compared with femora from patients with AFFs. Additionally, femora from patients without fractures trended toward greater diameter at 30 mm compared with those from both fracture groups (Fig. S1 and Table S1).

Microcomputed tomography (μCT) of the entire bone biopsies was used to assess the cortical microarchitecture. Bone from patients with atypical fractures had a smaller intracortical bone volume fraction compared with that from patients with typical fractures (Atypical −40% vs. Typical, $P = 0.03$). High-resolution μCT of the cortical microbeams that had undergone in situ fracture toughness testing was used to characterize the tissue microstructure at the crack tip. At this length scale, no differences in intracortical bone volume fraction, Haversian canal density, or Haversian canal diameter were observed between patient groups, likely reflecting that microbeams were necessarily cut preferentially from dense regions of cortex, excluding any large pores (greater than ∼100 μm), which significantly reduced the cross-section of the beam. Thus, whereas the whole-biopsy CT measures all cortical porosity, the microbeam CT measures only the porosity of a dense section of the cortex and does not include the large-scale porosity observed in the whole biopsies.

Bone Tissue from Patients with Atypical Fractures Has Elevated Mineral Content and Collagen Maturity Assessed by Vibrational Spectroscopic Imaging. To examine how the compositional properties of bone

Table 1. Patient characteristics for bisphosphonate-treated atypical fracture, bisphosphonate-treated typical fracture, bisphosphonate-treated nonfracture, bisphosphonate-naïve typical fracture, and bisphosphonate-naïve nonfracture groups

Characteristic	+BIS Atypical	+BIS Typical	+BIS Nonfx	−BIS Typical	−BIS Nonfx
No.	12	10	5	11	12
% female	100	100	100	100	100
Age, y, mean (SD)	72 (9.1)	81 (12)	75 (11)	83 (4.9)	71 (5.8)
Fracture morphology	12 atypical subtrochanteric	9 intertrochanteric 1 spiral subtrochanteric	N/A	10 intertrochanteric 1 spiral subtrochanteric	N/A
Bisphosphonate treatment duration, y, mean (SD)	8.2 (3.0)	7.7 (5.0)	6.4 (3.5)	N/A	N/A
Bisphosphonate treatment type	10 alendronate 2 ibandronate	5 alendronate 5 risedronate	2 alendronate 3 risedronate	N/A	N/A

N/A, not applicable.

tissue from patients with atypical fractures differed from those of the tissue from typically fractured or nonfractured patients, Raman and FTIR imaging were used. FTIR images were first analyzed to assess the means of four compositional parameters (mineral-to-matrix ratio, carbonate-to-phosphate ratio, collagen maturity, and crystallinity) across patient groups. Cortical bone from patients with atypical fractures had a greater mean mineralization compared with that from typical fracture patients and trended toward greater mean mineralization than that from nonfracture patients (Atypical +14% vs. Typical, $P = 0.03$; Atypical +11% vs. Nonfx, $P = 0.08$; Fig. 2). Cortical bone from patients with AFFs also had greater collagen maturity than that from patients without fractures and trended toward greater collagen maturity than that from patients with typical fractures (Atypical +11% vs. Typical, $P = 0.08$; Atypical +14% vs. Nonfx, $P = 0.04$).

Similarly to FTIR, Raman images of cortical bone were analyzed to compare the means of three compositional parameters (mineral-to-matrix ratio, carbonate-to-phosphate ratio, and crystallinity) across groups. Cortical bone from patients with atypical fractures had greater mean mineral-to-matrix ratio compared with that from typical and nonfracture groups (Atypical +15% vs. Typical, $P = 0.02$; Atypical +30% vs. Nonfx, $P < 0.01$; Fig. 2).

In addition, quantitative backscattered electron images were used to calculate the mean and peak values of the calcium distribution, Ca_{Mean} and Ca_{Peak}, respectively, for all patient groups. The quantitative backscattered electron imaging (qBEI) parameters did not differ across groups (Table S1).

Bone Tissue from Patients with Atypical Fractures Has Elevated Hardness. Once elevated tissue mineralization in bone tissue from atypical fracture patients was confirmed, nanoindentation was used to assess the nanomechanical properties at the same locations. Maps of nanoindentation points were analyzed to calculate the mean values of indentation modulus and hardness for all groups. Cortical bone from patients with atypical fractures had greater mean hardness than that from typically fractured and nonfractured patients (Atypical +18% vs. Typical, $P = 0.03$; Atypical +42% vs. Nonfx, $P < 0.01$), consistent with the elevated mineralization in the atypically fractured patient group (Fig. 2).

Bone Tissue from Patients with History of Long-Term Bisphosphonate Treatment Shows Elevated Mean Mineralization and Narrower Distributions of Nanomechanical Properties. To examine how the compositional properties of bone tissue from patients treated with bisphosphonates differs from that of bisphosphonate-naïve patients, Raman and FTIR imaging were used. Bone tissue from patients treated with bisphosphonates showed elevated mean mineralization assessed by both Raman and FTIR imaging. When compositional properties were assessed with FTIR imaging, cortical bone from patients treated with bisphosphonates had elevated mineralization compared with that from bisphosphonate-naïve patients (+BIS mineral:matrix +8% vs. −BIS, $P = 0.04$). When compositional properties were assessed with Raman imaging, cortical bone from bisphosphonate-treated patients had higher mean mineralization and trended toward lower mean crystallinity than that from bisphosphonate-naïve patients (+BIS mineral:matrix +13% vs. −BIS, $P = 0.02$; XST −2% vs. −BIS, $P = 0.08$). The observed greater mean mineralization in the cortices of patients treated with bisphosphonates is consistent with greater tissue maturity arising from reduced remodeling and consistent with previous studies showing changes in compositional properties of bone tissue from patients treated with bisphosphonates (17, 25).

When tissue mechanical properties were examined with nanoindentation, cortical tissue from patients treated with bisphosphonates had narrower distributions of hardness and modulus compared with cortical tissue from bisphosphonate-naïve patients (+BIS hardness FWHM −19% vs. −BIS, $P < 0.01$; modulus FWHM −17% vs. −BIS, $P = 0.05$; Fig. S2). Paralleling the compositional differences, these local mechanical differences are also consistent with reduced remodeling.

Bone Tissue from Patients with History of Long-Term Bisphosphonate Treatment Shows Lower Crack Initiation Toughness and Overall Toughness, with Less Crack Deviation. In situ fracture toughness testing in a variable-pressure scanning electron microscope allowed measurement of fracture toughness through crack-resistance curves (R-curves), which directly measure the fracture resistance properties, specifically the crack-initiation toughness and crack-growth toughness, of bone tissue. Cortical bone microbeams from patients treated with bisphosphonates had reduced crack-initiation toughness, assessed with the y-intercept of the R-curves (+BIS −79% vs. −BIS, $P = 0.01$) and decreased overall toughness (+BIS −23% vs. −BIS, $P = 0.03$) compared with those from bisphosphonate-naïve patients (Fig. 3). Additionally, cortical microbeams from patients without fractures had greater overall toughness compared with those from patients with typical or atypical fractures (Nonfx vs. Atypical, $P = 0.03$; Nonfx vs. Typical, $P = 0.05$; Fig. 3).

After fracture toughness testing, μCT scans of the cortical microbeams allowed evaluation of the crack path to assess the longer-range, extrinsic toughening generated by the interaction of the crack trajectory with respect to the bone microstructure. Specifically, tissue from bisphosphonate-treated patients trended toward cracks with lower tortuosity than that from bisphosphonate-naive patients (+BIS −40% vs. −BIS, $P = 0.10$; Fig. 4), indicating less deviation and deflection of crack paths, in particular involving less delamination along osteonal boundaries.

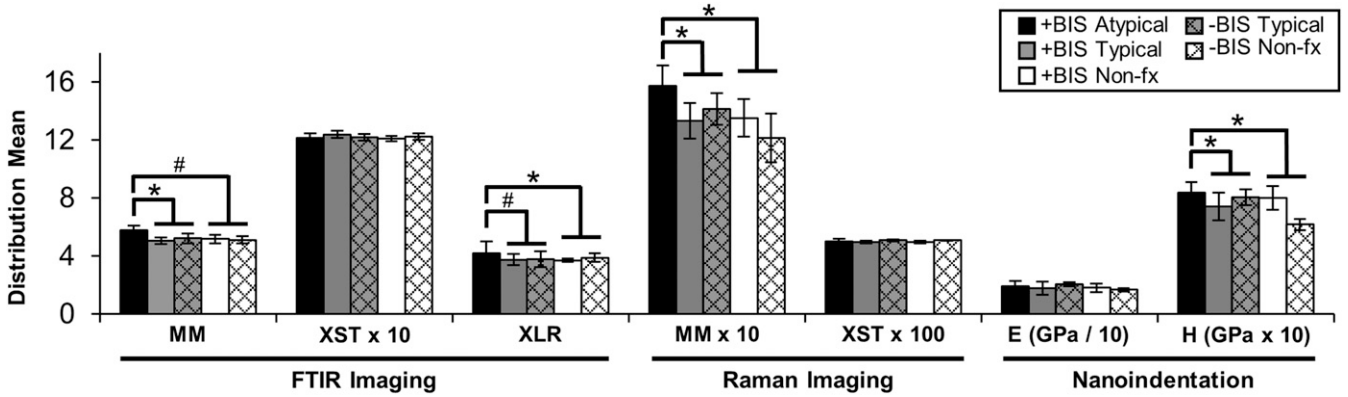

Fig. 2. Parameter means for compositional (mineral-to-matrix ratio, MM; collagen maturity, XLR; and crystallinity, XST) and nanomechanical (reduced modulus E; hardness H) properties, showing differences between cortical bone from bisphosphonate-treated (+BIS) or -untreated (−BIS) patients with atypical, typical, or no fracture. Data are shown raw (not age-adjusted), and only effects of fracture status (Atypical, Typical, or Nonfracture) that reached significance (*$P < 0.05$) or had a nonsignificant trend (#$P < 0.10$) are reported here. For a connecting letters report showing pairwise differences between all groups see Fig. S2.

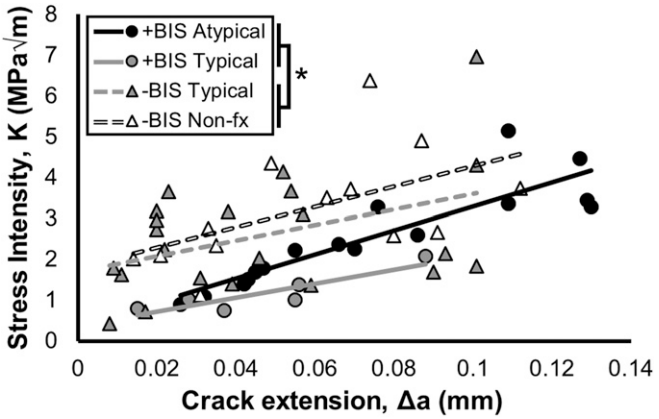

Fig. 3. Fracture resistance R-curves of stress intensity, K, as a function of crack extension, Δa, for all microbeams tested in in situ fracture toughness tests. Lines represent a fit of the data for each group. Tissue from patients treated with bisphosphonates (+BIS groups) was less tough than that from bisphosphonate-naïve patients (–BIS groups); $^{*}P = 0.01$. In addition, tissue from patients without fractures (–BIS Nonfx) was tougher than that from patients with typical or atypical fractures ($P = 0.03$ by linear fixed effects model).

Discussion

Summary. Since the first reports of AFFs the risk associated with long-term bisphosphonate treatment has become increasingly well-established (21, 22). However, the etiology of this rare fracture type and its causal relationship to bisphosphonate treatment was unknown. In the current study, using tissue from women who experienced AFFs after long-term bisphosphonate treatment, we have shown evidence that long-term bisphosphonate treatment acts to degrade the fracture-resistance toughening mechanisms inherent to healthy bone.

Loss of Intrinsic Toughening with Long-Term Bisphosphonate Treatment. Using in situ fracture toughness testing to measure crack propagation in cortical microbeams from bisphosphonate-naïve and bisphosphonate-treated patients (including those with AFFs), we report that bisphosphonate treatment reduces fracture toughness of cortical bone. In this study, analysis of tissue fracture toughness as a function of crack extension (R-curves) shows that bone tissue from patients treated with bisphosphonates has an overall decrease in the stress intensity required to propagate a crack, and decreased crack-initiation toughness, which indicates a deficit in intrinsic toughening mechanisms in bisphosphonate-treated bone (26, 27).

This finding is corroborated by the nanoscale compositional and mechanical data. Cortical bone from patients with atypical fractures had greater tissue mineral content as assessed by Raman and FTIR imaging and greater collagen maturity as assessed by FTIR imaging, as well as greater hardness, relative to that from patients without fractures, all of which are expected to diminish the ductility and hence decrease intrinsic toughness in bone (28). Consistent with these results, increased FTIR mineralization and collagen maturity are associated with increased fracture risk (29).

Clinically, AFFs often occur with prodromal pain and form a stress callus, indicating that they are likely stress fractures caused by fatigue loading (23, 24). The decreased crack-initiation toughness in combination with a higher degree of mineralization and reduced turnover due to bisphosphonate treatment is consistent with a fatigue fracture.

Loss of Extrinsic Toughening with Long-Term Bisphosphonate Treatment. In addition to decreases in crack-initiation toughness, tissue from patients treated with bisphosphonates had lower crack tortuosity than that from bisphosphonate-naïve patients, meaning that the cracks in these beams were less likely to split or delaminate along osteonal boundaries. Crack splitting, deflection, and twist are extrinsic toughening mechanisms that consume energy that would otherwise be used to propagate the crack forward, thereby decreasing the local stress intensity actually experienced at the crack tip, essentially doubling the fracture toughness of cortical bone (26, 30). The loss of this toughening mechanism in bisphosphonate-treated bone suggests that unlike in untreated bone, where highly mineralized cement line boundaries surrounding osteons represent the most favorable crack path, in bisphosphonate-treated tissue the greater homogenization of mineralization may lead to cement lines not acting as a boundary to direct transverse crack propagation, resulting in a corresponding loss in fracture resistance (30–32).

Clinically, AFFs are seen radiographically to have transverse, brittle fracture morphology, where the crack path cuts through the cortical osteonal structure, with minimal deviation. The observed reduction of crack deviation at osteons and decreased overall toughness in tissue from patients treated with bisphosphonates is consistent with this transverse, flatter fracture plane.

Relationship of Current Findings to Clinical Experience with Bisphosphonates and AFFs. The current work illuminates complex effects of bisphosphonates on bone tissue structure and mechanical

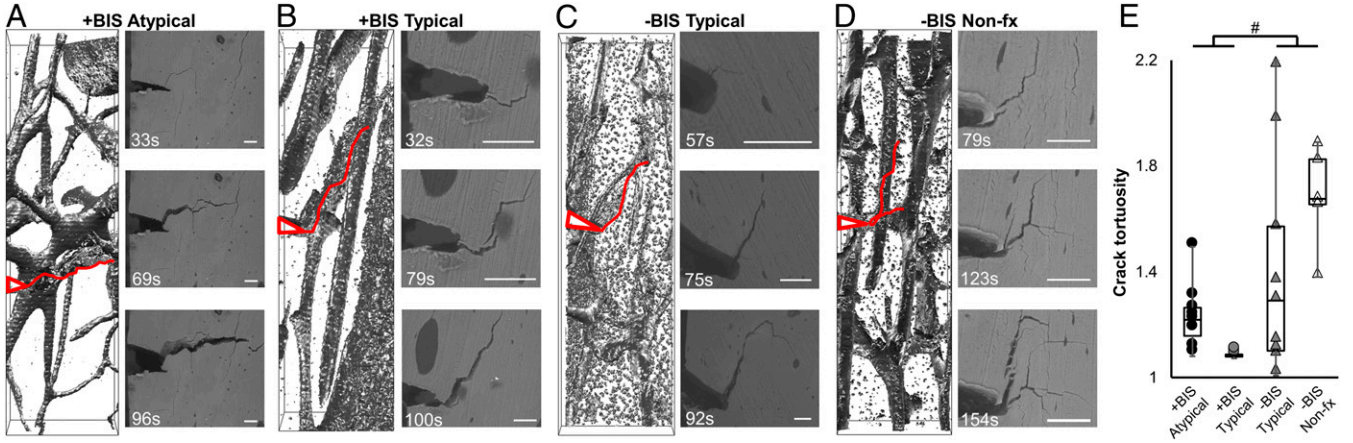

Fig. 4. Reconstructed microbeam μCT crack paths and SEM images of propagated cracks in cortical tissue, with notches and crack paths highlighted in red, from an (*A*) atypical fracture patient (+BIS Atypical), (*B*) a typical fracture patient with (+BIS Typical) and (*C*) without (–BIS Typical) history of bisphosphonate treatment, and (*D*) a patient without a history of fragility fracture or bisphosphonate treatment (–BIS Nonfx), showing (*E*) trend toward lower crack tortuosity in bisphosphonate-treated groups ($^{\#}P < 0.10$ by Mann–Whitney *U* test), suggesting less deviation at osteonal interfaces. (Scale bars, 50 μm.)

properties across multiple length scales. At the whole-bone scale, bisphosphonate treatment has long been known to reduce fracture risk by preventing postmenopausal bone loss and microarchitectural deterioration, reducing structural weakness at trabecular sites (11). At the millimeter to micro scales examined here, reductions in turnover with long-term bisphosphonate treatment contributed to decreased cortical resistance to crack propagation. The large reductions in fracture risk observed in clinical trials of bisphosphonates (4, 12) suggest that the macroscopic mechanisms promoting fracture reduction at trabecular sites dominate in the majority of patients; however, the microscopic mechanisms that promote fracture susceptibility in the cortex may be critical to the subset of patients at risk for AFFs. In addition, the durations of bisphosphonate treatment examined in the current study represent relatively long durations currently recommended only for patients at the highest risk of fracture (33); therefore, changes in tissue properties in response to shorter durations of bisphosphonate treatment are expected to be more moderate. Indeed, risk of AFFs seems to increase with treatment duration and decrease with cessation (21).

However, a patient's predisposition to experiencing an AFF depends on more factors than just reduced cortical toughening mechanisms: these rare fractures likely require the convergence of several disadvantageous events, representing a "perfect storm" of risk. First, increased curvature of the femoral diaphysis increases the cyclic mechanical loads on the lateral femoral cortex. Retrospective radiographic review demonstrated that patients with AFFs had greater femoral curvature than nonfracture controls, which would contribute to greater tensile stresses on the lateral cortices of the AFF patients (34). Next, reductions in toughening mechanisms in cortical bone, caused by long-term bisphosphonate treatment, or other genetic, pharmacologic, or metabolic factors, allow initiation and the start of propagation of a crack through the cortex. Finally, crack growth that outstrips healing is required for continued crack propagation. The incidence of "incomplete" AFFs in asymptomatic patients is much higher than that of complete catastrophic atypical fractures (35), suggesting that the majority of patients who experience a partial AFF may recover through healing of the incomplete fracture before it propagates.

Together, these lines of evidence suggest that reduced cortical toughness with bisphosphonate therapy is one of many factors contributing to AFFs. Identification of the subset of patients at risk for the confluence of these deleterious factors will assist in risk stratification of patients at greatest risk of AFFs (33).

This study has several important limitations and strengths. First, the sample size is relatively small because of the rarity of AFFs, which may limit statistical power. In addition, the cross-sectional study design prevents discernment of whether the observed differences in bone tissue properties in bisphosphonate-treated patients already existed in these patients before treatment. Finally, although AFFs do occur in bisphosphonate-naïve patients (6), none were observed in the 5 y during which patients for this study were enrolled; thus, the study lacked a bisphosphonate-naïve atypical fracture group. Despite these limitations, this study is an important step in understanding the etiology of AFFs. In particular, direct assessment of fracture properties of human biopsies taken adjacent to a clinically relevant fracture site allowed discernment of the effects of long-term bisphosphonate treatment on toughening mechanisms in bone tissue.

Conclusion. This study suggests that decreasing bone turnover through long-term antiresorptive treatment not only changes bone's nanoscale material properties but also affects toughness on the length scale of hundreds of micrometers through reductions in extrinsic and intrinsic toughening mechanisms. Despite this, the risk-to-benefit ratio of bisphosphonate treatment remains highly favorable for patients with osteoporosis (36). Thus, our work contributes to an evolving understanding of the complex effects of long-term bisphosphonate treatment on bone tissue properties and can inform guidelines for timing and duration of treatment for patients at risk for fracture.

Materials and Methods

Patient Cohort and Study Design. Postmenopausal women with (*i*) intertrochanteric and subtrochanteric femoral fragility fractures scheduled for open reduction and internal fixation using a cephalomedullary device (fracture groups) or (*ii*) osteoarthritis scheduled for total hip arthroplasty (nonfracture groups) were considered for inclusion. The following exclusion criteria were applied: high-energy traumatic fracture, prior fragility fracture, metabolic bone diseases (other than osteoporosis), hyperparathyroidism, bone metastasis, renal or hepatic failure, or history of treatment with bone-active agents other than bisphosphonates. Patients were allocated to groups (Table 1) based on fracture morphology and history of bisphosphonate use: bisphosphonate-treated atypical fracture (+BIS Atypical, $n = 12$); bisphosphonate-treated typical fracture (+BIS Typical, $n = 10$); bisphosphonate-treated nonfracture (+BIS Nonfx, $n = 5$); bisphosphonate-naïve typical fracture (−BIS Typical, $n = 11$); or bisphosphonate-naïve nonfracture (−BIS Nonfx, $n = 12$).

For patients with fractures, preoperative radiographs were evaluated in a blinded fashion to classify fractures as typical (intertrochanteric or spiral subtrochanteric) or atypical (6). For patients with fractures, 8-mm-diameter corticocancellous biopsies were collected during fracture repair from the lateral aspect of the proximal femur, at the insertion site for the spiral blade of the cephalomedullary device. For patients without fractures, identically sized biopsies were collected from an anatomically matched site. All procedures were approved by the institutional review boards of the Hospital for Special Surgery and New York-Presbyterian Hospital. All patients provided informed consent.

Biopsies were embedded in polymethyl methacrylate (PMMA). All biopsies were analyzed by FTIR imaging, Raman imaging, nanoindentation, and whole-biopsy μCT. A subset (total $n = 40$; +BIS Atypical $n = 7$; +BIS Typical $n = 9$; −BIS Typical $n = 11$; +BIS Nonfx $n = 2$; −BIS Nonfx $n = 11$) were analyzed with qBEI (*Supporting Information*). All biopsies that had a rectangular section of cortex with minimum dimensions of $5 \times 0.5 \times 0.5$ mm undamaged by retrieval underwent fracture testing (total $n = 21$; +BIS Atypical $n = 6$; +BIS Typical $n = 3$; −BIS Typical $n = 7$; +BIS Nonfx $n = 0$; −BIS Nonfx $n = 5$). The bisphosphonate-treated nonfracture group was not included in microbeam analyses, because this group had no biopsies with sections of cortex large enough to excise an undamaged microbeam.

Radiographic Analysis. Cortical thicknesses were measured from the postoperative radiographs of the fractured femur at 30 mm and 100 mm distal to the lesser trochanter. Cortical ratio was calculated as the ratio of medial and lateral cortical thickness to the total diameter.

FTIR Imaging. For each biopsy FTIR images were collected from three nonconsecutive 1-μm-thick sections with an FTIR imaging system (Spotlight 400; Perkin-Elmer) over the range of 800–2,000 cm^{-1} with a spatial resolution of ~6.25 μm (17), to obtain the mineral-to-matrix ratio, carbonate-to-phosphate ratio, collagen maturity (XLR), and the mineral crystallinity (XST). For each FTIR image, the values of each calculated parameter were used to generate a distribution, which was used to calculate the mean, and fit with a Gaussian curve to calculate the FWHM for each parameter.

Raman Imaging. Each PMMA-embedded bone biopsy was polished (37), and three cortical and three trabecular regions of 400 μm × 400 μm were imaged with a Raman imaging system (InVia Confocal Raman Microscope; Renishaw Inc.). Spectra were collected with a spacing of 50 μm. over the range 800–1,800 cm^{-1} with a 785-nm laser collecting for 90 s at 50% power with cosmic ray correction. Each spectrum was baseline-corrected, normalized to the absorbance of PMMA at 813 cm^{-1}, and had the PMMA contribution subtracted (MATLAB; MathWorks). Data that were collected from an area of PMMA, had significant contribution from cosmic rays, or that had a low signal-to-noise ratio were excluded. For each spectrum, three experimental outcomes were calculated: mineral-to-matrix ratio (area ratio of phosphate ν_1 and amide III), carbonate-to-phosphate ratio (area ratio of carbonate ν_1 to phosphate ν_1), and mineral crystallinity (the inverse of the FWHM of a Gaussian fit of the phosphate ν_1 peak) (38).

Nanoindentation. Nanoindentation (TriboIndenter; Hysitron) was performed with a Berkovich tip loaded at 100 μN/s, held at 1,000 μN for 10 s, and unloaded at 100 μN/s, on the same points where Raman measurements were taken. Measurement locations were aligned using an alignment grid on each sample surface, as well as fiducial markers. The unloading curve of each indent was analyzed to find the hardness and reduced modulus (39). Optical images were used to exclude indents that fell on PMMA.

In Situ Fracture Toughness Testing. Microbeams of cortical bone were machined from PMMA-embedded biopsies, such that the bone tissue was exposed on the beam surface, and polished to final dimensions ~5 mm × 0.5 mm × 0.5 mm. PMMA

contributes minimally to fracture toughness measurements of hydrated samples (40). A sharp notch was introduced into the beam with a razor blade irrigated with 1-μm-particle-size alumina slurry. The PMMA-embedded microbeams were then rehydrated in HBSS for 2 h before testing (at which point they were fully rehydrated, as assessed by a plateau in their weight following placement in HBSS). The rehydrated microbeams were tested in situ in a variable-pressure scanning electron microscope (Hitachi S-4300SE/N; Hitachi America) in three-point bending using a 2-kN bending stage (MicroTest; Gatan) with a loading span, S, of 2 mm and a displacement rate of 0.55 μm/s. Crack initiation and extension were imaged during testing; force-displacement data were recorded simultaneously. Crack-resistance curves (R-curves) were determined in general accordance with the current nonlinear-elastic J-based ASTM Standard E1820-15a for the measurement of fracture toughness (41), which incorporates the role of plastic deformation in the determination of the material's resistance to failure (*Supporting Information*).

3D Morphometric Assessment via μCT. μCT scans (Xradia VersaXRM-520; Zeiss) of the postfracture-toughness-testing microbeams was performed at a voxel size of 1–1.6 μm, giving a field of view of 1 mm^3 around the crack tip. Samples were scanned in PBS. Reconstructed grayscale slices of the 3D data were used to threshold and segment the microbeam image with MATLAB. The segmented data were used to calculate intracortical bone volume fraction, Haversian canal density, and Haversian canal diameter (BoneJ; NIH).

μCT images were also used to find the crack path and analyze its direction relative to the osteonal orientation within the microbeams. Crack tortuosity was calculated as the average ratio of crack length (measured in ImageJ by tracing the crack path) to chord length (measured as the straight line length from notch tip to the tip of the crack) across six 2D longitudinal cross-sections that spanned the width of each microbeam.

Statistical Analysis. For all demographic, compositional, and nanomechanical measures a nonparametric linear fixed effects model with Mann–Whitney U post hoc ($\alpha = 0.05$) was used to examine differences across groups, isolate the effects of bisphosphonate treatment and fracture morphology, and adjust for patient age. For R-curve analysis, both fixed effect linear and linear mixed models were used to assess the differences in R-curves across groups, with a Mann–Whitney U post hoc test ($\alpha = 0.05$). Statistical analysis was performed with R (42). Data are available on request.

ACKNOWLEDGMENTS. We thank Dr. Mathias Bostrom and Dr. Charles Cornell for assistance with obtaining biopsies, Dr. Michael Hahn for technical support, and Amy Cao and Carmen Ngai for collection and analysis of Raman data. This work was supported by NSF Civil, Mechanical and Manufacturing Innovation Grant 1452852 and an American Society for Bone and Mineral Research Junior Faculty Osteoporosis Research Award (to E.D.), and the German Research Foundation (DFG) under Grant BU 2562/2-1/3-1 (to B.B.). This material is based upon the work supported by an NSF Graduate Research Fellowship (to A.A.L.) under Grant DGE-1144153. This work made use of the Cornell Center for Materials Research Shared Facilities, which are supported through the NSF Materials Research Science and Engineering Centers program (Grant DMR-1120296).

1. Kavanagh KL, et al. (2006) The molecular mechanism of nitrogen-containing bisphosphonates as antiosteoporosis drugs. *Proc Natl Acad Sci USA* 103:7829–7834.
2. Eastell R, Walsh JS, Watts NB, Siris E (2011) Bisphosphonates for postmenopausal osteoporosis. *Bone* 49:82–88.
3. Clézardin P, Benzaïd I, Croucher PI (2011) Bisphosphonates in preclinical bone oncology. *Bone* 49:66–70.
4. Black DM, et al.; Fracture Intervention Trial Research Group (1996) Randomised trial of effect of alendronate on risk of fracture in women with existing vertebral fractures. *Lancet* 348:1535–1541.
5. Harris ST, et al.; Vertebral Efficacy With Risedronate Therapy (VERT) Study Group (1999) Effects of risedronate treatment on vertebral and nonvertebral fractures in women with postmenopausal osteoporosis: A randomized controlled trial. *JAMA* 282:1344–1352.
6. Shane E, et al.; American Society for Bone and Mineral Research (2010) Atypical subtrochanteric and diaphyseal femoral fractures: Report of a task force of the American Society for Bone and Mineral Research. *J Bone Miner Res* 25:2267–2294.
7. Shane E, et al. (2014) Atypical subtrochanteric and diaphyseal femoral fractures: Second report of a task force of the American Society for Bone and Mineral Research. *J Bone Miner Res* 29:1–23.
8. Khosla S, Shane E (2016) A crisis in the treatment of osteoporosis. *J Bone Miner Res* 31: 1485–1487.
9. Jha S, Wang Z, Laucis N, Bhattacharyya T (2015) Trends in media reports, oral bisphosphonate prescriptions, and hip fractures 1996-2012: An ecological analysis. *J Bone Miner Res* 30:2179–2187.
10. Kolata G (June 1, 2016) Fearing drugs' rare side effects, millions take their chances with osteoporosis. *NY Times*.
11. Rodan GA, Fleisch HA (1996) Bisphosphonates: Mechanisms of action. *J Clin Invest* 97: 2692–2696.
12. Cummings SR, et al. (1998) Effect of alendronate on risk of fracture in women with low bone density but without vertebral fractures: Results from the Fracture Intervention Trial. *JAMA* 280:2077–2082.
13. Launey ME, Buehler MJ, Ritchie RO (2010) On the mechanistic origins of toughness in bone. *Annu Rev Mater Res* 40:25–53.
14. Acevedo C, et al. (2015) Alendronate treatment alters bone tissues at multiple structural levels in healthy canine cortical bone. *Bone* 81:352–363.
15. Bajaj D, Geissler JR, Allen MR, Burr DB, Fritton JC (2014) The resistance of cortical bone tissue to failure under cyclic loading is reduced with alendronate. *Bone* 64:57–64, and erratum (2016) 83:283.
16. Zimmermann EA, et al. (2016) Intrinsic mechanical behavior of femoral cortical bone in young, osteoporotic and bisphosphonate-treated individuals in low- and high energy fracture conditions. *Sci Rep* 6:21072.
17. Donnelly E, et al. (2012) Reduced cortical bone compositional heterogeneity with bisphosphonate treatment in postmenopausal women with intertrochanteric and subtrochanteric fractures. *J Bone Miner Res* 27:672–678.
18. Tai K, Dao M, Suresh S, Palazoglu A, Ortiz C (2007) Nanoscale heterogeneity promotes energy dissipation in bone. *Nat Mater* 6:454–462.
19. Tang SY, Allen MR, Phipps R, Burr DB, Vashishth D (2009) Changes in non-enzymatic glycation and its association with altered mechanical properties following 1-year treatment with risedronate or alendronate. *Osteoporos Int* 20:887–894.
20. Odvina CV, et al. (2005) Severely suppressed bone turnover: A potential complication of alendronate therapy. *J Clin Endocrinol Metab* 90:1294–1301.
21. Schilcher J, Michaëlsson K, Aspenberg P (2011) Bisphosphonate use and atypical fractures of the femoral shaft. *N Engl J Med* 364:1728–1737, and erratum (2011) 365:1551.
22. Abrahamsen B, Eiken P, Eastell R (2009) Subtrochanteric and diaphyseal femur fractures in patients treated with alendronate: A register-based national cohort study. *J Bone Miner Res* 24:1095–1102.
23. Lenart BA, Lorich DG, Lane JM (2008) Atypical fractures of the femoral diaphysis in postmenopausal women taking alendronate. *N Engl J Med* 358:1304–1306.
24. Neviaser AS, Lane JM, Lenart BA, Edobor-Osula F, Lorich DG (2008) Low-energy femoral shaft fractures associated with alendronate use. *J Orthop Trauma* 22:346–350.
25. Roschger P, et al. (2001) Alendronate increases degree and uniformity of mineralization in cancellous bone and decreases the porosity in cortical bone of osteoporotic women. *Bone* 29:185–191.
26. Nalla RK, Kinney JH, Ritchie RO (2003) Mechanistic fracture criteria for the failure of human cortical bone. *Nat Mater* 2:164–168.
27. Nalla RK, Stölken JS, Kinney JH, Ritchie RO (2005) Fracture in human cortical bone: Local fracture criteria and toughening mechanisms. *J Biomech* 38:1517–1525.
28. Currey JD, Brear K, Zioupos P (2004) Notch sensitivity of mammalian mineralized tissues in impact. *Proc Biol Sci* 271:517–522.
29. Gourion-Arsiquaud S, et al. (2009) Use of FTIR spectroscopic imaging to identify parameters associated with fragility fracture. *J Bone Miner Res* 24:1565–1571.
30. Koester KJ, Ager JW, 3rd, Ritchie RO (2008) The true toughness of human cortical bone measured with realistically short cracks. *Nat Mater* 7:672–677.
31. Burr DB, Schaffler MB, Frederickson RG (1988) Composition of the cement line and its possible mechanical role as a local interface in human compact bone. *J Biomech* 21:939–945.
32. Yeni YN, Norman TL (2000) Calculation of porosity and osteonal cement line effects on the effective fracture toughness of cortical bone in longitudinal crack growth. *J Biomed Mater Res* 51:504–509.
33. Adler RA, et al. (2016) Managing osteoporosis in patients on long-term bisphosphonate treatment: Report of a task force of the American Society for Bone and Mineral Research. *J Bone Miner Res* 31:16–35, and erratum (2016) 31:1910.
34. Sasaki S, Miyakoshi N, Hongo M, Kasukawa Y, Shimada Y (2012) Low-energy diaphyseal femoral fractures associated with bisphosphonate use and severe curved femur: A case series. *J Bone Miner Metab* 30:561–567.
35. La Rocca Vieira R, et al. (2012) Frequency of incomplete atypical femoral fractures in asymptomatic patients on long-term bisphosphonate therapy. *AJR Am J Roentgenol* 198:1144–1151.
36. Black DM, et al.; Fracture Intervention Trial Steering Committee; HORIZON Pivotal Fracture Trial Steering Committee (2010) Bisphosphonates and fractures of the subtrochanteric or diaphyseal femur. *N Engl J Med* 362:1761–1771.
37. Donnelly E, Baker SP, Boskey AL, van der Meulen MCH (2006) Effects of surface roughness and maximum load on the mechanical properties of cancellous bone measured by nanoindentation. *J Biomed Mater Res A* 77:426–435.
38. Akkus O, Adar F, Schaffler MB (2004) Age-related changes in physicochemical properties of mineral crystals are related to impaired mechanical function of cortical bone. *Bone* 34:443–453.
39. Oliver WC, Pharr GM (1992) An improved technique for determining hardness and elastic modulus using load and displacement sensing indentation experiments. *J Mater Res* 7:1564–1583.
40. Busse B, et al. (2013) Vitamin D deficiency induces early signs of aging in human bone, increasing the risk of fracture. *Sci Transl Med* 5:193ra88.
41. ASTM International (2015) E1820-15a standard test method for measurement of fracture toughness (ASTM International, West Conshohocken, PA).
42. R Core Team (2017) R: A language and environment for statistical computing (R Foundation for Statistical Computing, Vienna).
43. Hengsberger S, Kulik A, Zysset P (2002) Nanoindentation discriminates the elastic properties of individual human bone lamellae under dry and physiological conditions. *Bone* 30:178–184.
44. Boskey AL, et al. (2016) Examining the relationships between bone tissue composition, compositional heterogeneity, and fragility fracture: A matched case-controlled FTIRI study. *J Bone Miner Res* 31:1070–1081.